3D Structural Modeling Using Remote Sensing and Ground-Based LIDAR

Ryan T. Coppersmith
Advisor: Dr. Christopher D. Connors
May 29, 2006
Department of Geology
Washington and Lee University
Lexington, VA

TABLE OF CONTENTS

Abstract

High-resolution remote sensing data and 3D modeling techniques offer new tools for structural analysis that improve on the efficiency, accuracy and precision of geologic mapping, and provide insight into the structure of an area that is difficult to obtain otherwise. I combine conventional remote sensing data and geologic mapping with laser survey data into a complete 3D model that constrains the surface and subsurface geometry of a part of the Catalan Coastal Range at the edge of the Ebro Basin, Spain.

For lower relief areas two approaches are used to interpret orthophotos: I interpret on orthophotos in map view and then visualize the interpretation in 3D by draping the interpretation and photos over digital elevation models, secondly I interpret directly on the draped orthophotos. I find the latter approach to be much more accurate in interpreting the surface geology. In areas that are impossible to map in a conventional sense with any precision, such as vertical cliff faces 100's of meters high, I employ 20 cm resolution ground-based LIDAR. These data are of such high fidelity that surfaces generated from the scans allow delineation of individual beds that can be interpreted directly on the surface in 3D, similar to interpreting draped orthophotos as discussed above.

To extend the surface interpretation into the subsurface I use a technique exploiting the local 3D information of surface contacts with cross section construction to ultimately build a self-consistent 3D model. For surface contacts that have demonstrable relief change, a shallow subsurface 3D model is created. These provide local structural control for cross-section construction. The cross sections are then used as a framework for building of a 3D model. I found that making use of

surface data in a 3D environment such as that described above provides additional understanding of the structure of an area than cannot be obtained by conventional mapping alone.

Introduction

Tectonic Setting

The Catalan Coastal Ranges are located in Northeast Spain on the southeastern side of the Ebro Basin, Spain. The Catalonian Coastal Range is one of the three contractional thrust belts formed from the early Eocene to Oligocene convergence of the Iberian plate (Iberian Peninsula) and Eurasian plates (Jones et al., 2004). The range stretches 250 km long and about 30 km wide. The formation of the Catalans coincided with the formation of the Pyrenees to the north and with the Iberian range to the southeast forming a triangle around the Ebro Basin (Figure 1). During deformation Oligocene conglomerates filled the foreland basin and overlapped the mountain range, developing substantial growth strata. Since then Plio-Pleistocene fluvial systems have drained from northeast to southeast, eroding away most of the Tertiary in the hinterland and exposing the fold and thrust belt.

Regional Geology

Lawton et al., (1999) and Jones et al., (2004) have compiled stratigraphic columns of areas near Horta de San Joan and Grandesa respectively. The exposed units consist of Triassic to Cretaceous carbonates and shales transitioning unconformably to basin deposits of Tertiary sediments. These sediments represent coarse, bedload-dominated streams and alluvial fans as material was transported from

the rising thrust belt to the basin (Cabrera et al., 1985; Jones, 2004). While the columns from Lawton and Jones differ slightly in thicknesses for both Mesozoic and Tertiary units, this is not surprising. Lopez et al. (1985) constructed a geologic map that has been the basis of our study in viewing the geology of the area (Figure 2). The fold and thrust belt shows repeating sections in the hinterland with the oldest unit in the lower Triassic. This suggests a detachment in the T2 Muschelkalk formation which will be discussed later in more detail.

Goals

The main goal of this project was to capture the subsurface geometry of the fold and thrust belt by constructing a well constrained 3D model which provides insight into the structure of an area, an improvement of serial conventional cross sections. After a model of the subsurface is completely built it is possible to predict the timing of faulting and folding. To achieve these goals four regional cross sections were constructed that are all laterally aligned.

To achieve a well-constrained subsurface model of the mountain range many approaches were used. The first approach was to integrate all of the data into a 3D environment using Esri's ArcGIS 8.3 (2002), and Gocad 2.0.8 (2003). Next, I extracted near-surface 2D data along our regional surface profiles. These data were moved into Deneba's Canvas X (2005) where the 2D cross sections could be extended to depth. The last process was bringing the data back into Gocad in order to make a 3D model of the structure of the mountain range.

Stratigraphy, Thicknesses and Regional Dip

Stratigraphic Thicknesses

Lawton et al., (1999) and Jones et al., (2004) have compiled stratigraphic columns of areas near Horta de San Joan and Grandesa respectively (Figure 7). It is quite clear that their columns have varying thicknesses in the upper Jurassic, as well as in the Triassic. This is reasonable due to the Jurassic thickening towards the southeast. Both stratigraphic columns are very similar and suggest a detachment in the lower Triassic (T2) Muschelkalk formation.

In constructing my own stratigraphic thickness for the study area, both of the previous columns were taken into consideration (Figure 8). Since the stratigraphic thicknesses can vary somewhat dramatically from region to region, it was important to look at local thicknesses obscured in the digital data. Distances between the interpreted subsurface were compared to the two existing columns. Many were similar, with slight variations in the J8 units, along with the Tertiary. Further, all of the Mesozoic thicknesses were compared to those of Cabrera (1985), along with Dewhurst (2005). In my region I found the Mesozoic to be laterally continuous, maintaining layer thickness through all four sections.

Detachment

The fold and thrust belt of the Catalan Coastal Range displays imbricate sections of Mesozoic carbonates that have been thrust up from depth. Lower Triassic (T3) to upper Jurassic (J11) is commonly seen in consecutive thrust sheets. This alone suggests a detachment that is allowing rocks from depth to ride to the surface. The

very earliest Triassic (T2) only outcrops in one location in our study area. The T2 formation is composed of limestone with interbedded evaporites. Since detachments commonly form along evaporite layers, and since T2 outcrops only once in the region, this suggests a regional detachment. The T2 Muschelkalk formation has approximately 1.5 kilometers of overlying strata on average (Figure 8). There is a maximum of 95 meters in the T2 unit until the proposed detachment level. Stratigraphy from Jones et al. (2004), Lawton et al. (1999), Sole de Porta et al. (1987), Salvany et al.(1987) all confirm a regional detachment in the Muschelkalk formation. Further, the Pyrenees to the north experiences the same detachment as well (Calvet et al., 1987). While our depth to detachment varies slightly, this is due to differences in Tertiary and/or Mesozoic variations.

Repeated sections at high frequencies in the hinterland suggest an imbricate system. The imbricates are clearly detaching from an upper detachment as seen by the faults running parallel to bedding and following contour lines. Upper detachments are seen in the Cretaceous and in the upper J8 where the Cretaceous is missing, which is not seen in our section. The thrusts in the hinterland could not possibly all be detaching from the Muschelkalk detachment because their vertical displacements are limited by the spectral dip domain, which will be explained in the Cross Section Construction chapter.

Tertiary thickness

The Tertiary sediments in the Catalans represent coarse, bedload-dominated streams and alluvial fans as material was transported from the rising thrust belt to the basin (Cabrera et al., 1985; Jones, 2004). The Catalan Coastal Range combines well-

exposed, syntectonic sedimentation (growth strata) associated with fault-related folding (Burbank et al.,1996). The upper Tertiary, T23 unit, has well exposed growth strata in the foreland, along with at Roca de Benet. The Tertiary sediments were deposited onto uneven erosional surfaces, usually uncomformably on top of Mesozoic carbonates. Many times they were deposited as alluvial fans, or by fluvial systems which causes thicknesses to vary laterally, especially when looking at them at a local scale. In our study area the lower T21 sediments thin from the northeast to the southeast. Further, the T23 sediments thin from the southeast to the northeast. The Tertiary thicknesses were measured in 2D where the Tertiary units are exposed to the northeast of the sections. For lack of better constraint, we allowed the thinning in opposite directions to cause the detachment to be at equal depths in all four sections, in the undeformed state.

Regional Dip

During the formation of a mountain range, flatlying strata is deformed and stacked during shortening. The hinterland experiences large amounts of thickening that produces flexure due to loading. The geometry of the flexed, but otherwise undeformed strata is known as a regional dip. The hinterland in this region has been calculated by taking beds that appear to have been flatlying and finding the dip. The regional dip for the hinterland has been calculated to 0.7 degrees towards the hinterland.

During and after deformation, sediments are eroded from the mountain range and deposited into the foreland basin. This produces a regional dip due to loading and flexing of the foreland. The foreland basin was calculated to be experiencing a

0.6 degree dip towards the foreland. Although this dip seems small, it can make a large difference at the kilometer scale. For example, a regional dip that travels horizontally for 10 km, would make the strata about 104 m deeper than it would be assuming no regional dip.

Data Collection and Methods

The existing data for the research includes a 1:50,000 geologic map (López et al. 1985) from the Instituto Geológico y Minero de España, Digital Line Graphs, 1:5,000 orthorectified airphotos, Ground Based LIDAR, and conventional field mapping measurements. With the combination of ArcGIS, Gocad and Canvas, I was able to create a 3D model of the subsurface of the Catalan Coastal Range.

GIS Method

The local 1:50,000 geologic map served as the primary geologic contacts. By scanning and orthorectifying the map it was exported as a geotiff image. As such, it was brought into ArcGIS suite to digitize each contact as a different polyline shapefile. In order to be useful as surfaces in a 3D model, the shapefiles represent base contacts for each unit. Faults were also digitized. Most of this work was done by Dewhurst (2005).

ArcScene was used to build TINs (Triangulates Integrated Network) from the Digital Line Graphs by both Dewhurst (2005) and myself in this study. The 1:5000 orthophotos were then draped over the TIN to give the orthophoto a 3D topography. The primary contacts digitized in the 2D ArcMap were then draped in a similar way into 3D. The contacts clearly did not all line up correctly (Figure 3). These were due

to mapping errors, along with errors in the draping process. Accuracy of the contacts was very important since they were used as the surface constraints in creating cross sections.

To correct for these contact errors ArcMap and ArcScene were used simultaneously. Editing the contacts could only be done in 2D, but were easier to view in 3D. Therefore, incorrect contacts were viewed in ArcScene where it was possible to see bedding planes with the high resolution orthophotos. Once the contact or fault was reinterpreted, it was edited in ArcMap (Figure 4).

The Tertiary sediments in the foreland proved to be an important constraint as well. Due to the contacts being very close together in the hinterland, there were plenty of surface attitudes to constrain this part of the mountain range. However, in the foreland where the topography flattens, the contacts were very far apart, leaving little constraint. The ArcGIS method worked wonderfully in finding and digitizing Tertiary beds that could later be used to constrain the foreland.

Field Methods

Although remote sensing techniques proved to be helpful and accurate, a few problems still remained. Steep topography resulted in no data in 3D due to stretching a 2D airphoto onto a 3D TIN. This left us with no constraints on Roca de Benet, a prominent Tertiary structure that displays excellent growth strata while sitting uncomformably over Jurassic carbonates (Figure 5). The importance of this structure will be explained later, however, it is important to understand that the bedding of the growth strata must be well-constrained to capture the fanning of dip that it displays. To do this a ground based LIDAR (Light Distance and Ranging) system known as

Optech ILRIS 3D (Optech, 2004) laser imager was used, to make a 3D image of Roca de Benet (Connors, 2004; Dewhurst 2005; Coppersmith, 2005). This instrument involves going into the field and taking images of the structure from multiple angles (Coppersmith et al., 2005). The multiple images were stitched together in a 3D environment by Chris Connors using Polyworks (InnovMetric, 2005) to create a 360 degree model of the structure.

The surface contacts were checked and corrected for in the field. Areas of uncertainty while remotely mapping, hidden areas, and fault zones were all remapped in the field. Numerous strike and dip measurements were taken and later brought into the 3D environment. Surface attitudes from Lawton et al. (1999), along with Lopez et al. (1995) were brought into the program as well.

Gocad Methods

Our next method used Gocad, a completely 3D environment that can handle large datasets and offers excellent visualization capabilities. All data were extracted from ArcGIS and imported into Gocad. The LIDAR data was brought directly into Gocad. With the corrected contacts draped onto the orthophotos, surfaces were produced from the contacts. Contacts draped on 3D topography produce a surface orientation when viewed in 3D. From this surface orientation Gocad is capable of fitting a convex hull around the contact. The hull is manually fit to the orientation of the contact and interpolated to the contact as a 3D surface. These surfaces are a preliminary interpretation of the subsurface. More importantly, these surfaces provide a surface attitude for the cross section that will eventually be created by

extending the surfaces to depth. First, surfaces are constructed for every contact and fault (Figure 6).

Regional Cross Sections

Extracting 2D data from 3D

With all of the data loaded into Gocad, the surfaces constructed from the contacts and faults were used to build regional cross sections (Figure 9). First, the 3D data must be extracted into 2D data to begin a 2D cross section. To do this, the four cross sections were made into surface profiles by intersecting a vertical plane with the topography. The result is a polyline that is a surface profile for each of the four sections. Surface attitudes, also known as tadpoles, were made to show the dip of each contact, or Tertiary bed, on the surface profile. This was done by creating a vertical plane along the same plane as the surface profile. Where the contact surfaces intersected the vertical plane I created a polyline in Gocad which is the orientation of the surface at that point. After doing this for every surface, fault, or Tertiary bed, each surface profile had numerous surface attitudes. This is where the mapping of the Tertiary bedding was very helpful. While the hinterland had plenty of constraints from contacts, the foreland was lacking in this sense. Our field measurements, along with Lawton et al. (1999), and Lopez (1995), were put into Gocad as small surfaces and used in an identical way.

Extending to Depth

The surface profiles with their respective tadpoles were moved from Gocad into Canvas, a 2D environment. This is difficult due to Gocad working in real-world

X,Y, and Z coordinates while Canvas works in X, Y space. Using a Matlab code developed by Chris Connors (Appendix I). I was able to translate and rotate the data to a convenient and consistent location within Canvas. I had to be sure not to move the data once in Canvas in order to eventually move it back to its original location in Gocad.

Cross Section Techniques

Before extending the surface attitudes to depth there are certain techniques for constructing a cross section. If beds are carelessly extended to depth, the result will not compensate for all beds and the section will not be balanced. I am assuming that the fold and thrust belt stratigraphy mostly conserves layer thickness. This seems reasonable since repeating sections display similar layer thicknesses as one moves from the foreland to the hinterland. Other than possible local variations due to smaller scale deformation, thickness remains constant. The exception to this is growth strata along with detachment fold cores. A second technique used to construct the sections is the kink-band method (Suppe, 1985). The kink-band method allows for an axial surface to constrain the subsurface geometry while conserving layer thickness between units and also honoring surface data. Every fold shape could be determined if the fault shape is known, and vice-versa, using an equation for fault bend folds (Suppe, 1985). In imbricate systems such as those in the hinterland, it is necessary to account for refolding of a previous fault ramp. Using Suppe (1983) along with Shaw et al. (2005) for reference, the spectral-dip-domain method calculates the dip domain of any fault ramp, as long as the initial step up angle is known. The theory describes the increases in dip order caused by refolding of

shallow thrust sheets by younger and deeper faults (Shaw et al., 2005). Lastly, the stratigraphic column of undeformed thicknesses was used as a background template. This was also done with a local part of the geologic map in order to quickly view as a reference.

Cross Section Observations

Cross section D-D' contains a large anticline in the foreland that extends to flat towards the basin (Figure 10). The anticline is asymmetrical with very steeply dipping beds in the forelimb, greater than 60 degrees in some places. The first thrust fault extends to depth from a fourth order dip to flat where it meets the second thrust fault further in the hinterland, creating a splay. Further in the hinterland an imbricate system steps up from the major thrust.

Cross Section C-C' displays a southeast plunge of the anticline that was prevalent in the D-D' foreland and is now a minor fold (Figure 11). The local detachment below the Tertiary is consistent in this section. Notice that the most foreland thrust fault is displacing within the J7 unit, a second local detachment seen in all four sections. The second most foreland fault displaces along this same unit. The imbricate system in the hinterland displaces along the lower Triassic in all four sections, consistent with the major regional detachment.

Cross section B-B' is very similar to the foreland of A-A' and C-C' with two minor folds being the extent of foreland deformation before flattening towards the basin (Figure 12**).** The most foreland thrust fault extends to depth from fourth order dip to flat. However, it is clear that the units are folded. This is caused by a late deep thrust fault that refolds everything above it. Using Shaw et al., (2005) folding

vectors, the folding of the overlying material was calculated by using the amount of folding from the deep fault bend fold and translating that to the upper thrust sheets.

Cross section A-A' has a near identical foreland to B-B' along with a refolded splay due to a late, deep thrust fault (Figure 13). This section shows especially well the break-forward imbricate system in the hinterland. First order through fourth order fault dips are seen in the four corresponding imbricate thrust faults.

Creating a 3D Model

Moving 2D data to 3D

In order to create the 3D model the 2D cross sections were taken from Canvas into Gocad. To do this the cross sections were exported as shapefiles and changed to plines with Matlab code written by Connors (2006) (Appendix II). The cross sections were translated and rotated into their original positions in Gocad. This was done separately for each of the four cross sections.

Creating the Model

Once the cross sections are in place, the 3D model was made by creating surfaces that connect the sections. Gocad has a tool that can create a surface from several polylines. To see the model clearly, only a few units were selected. In this case (Figure 14a-e) all of the faults were created into one surface, along with some Tertiary, Jurassic and Triassic units. Once the model is created, the deformed beds are seen in a lateral sense. This allows obvious problems to be seen and fixed. Some of these problems include misaligned folds, faults, and changes in layer thickness where it should be conserved. This provides an iterative approach to eventually

balancing the cross sections. Once the problem is recognized it can be changed in 2D and moved back into the 3D model. This technique is not possible with 2D cross sections alone. The 3D model provides a further understanding to how the sections vary along strike.

Results and Interpretation

Cross Section Implications

Surface attitudes were extended to depth with the previous methods. Cross sections A-A' to D-D' correspond laterally from southeast to northeast. The first step is extending the forelands to depth. Since the forelands are the least deformed, and contain the fewest faults, this acts as a pin, holding the front part of the section still.

When constructing cross sections that sit very close laterally it is important and difficult to think in a three dimensional way. Any fold or fault interpreted on one section will most likely be present in the next section. The plunging of folds and thickening of units are very important in a 3D environment and were taken into great consideration while building the sections.

The timing of the thrust faults in the sections was constrained by indicators found within my data. The second most foreland thrust cut across section and therefore came after the one in front of it. The repeating sections in the hinterland came from a detachment of 1.5 km, and could be explained by an imbricate system. Multiple thrusts simply could not bring units that far up due to being limited by the spectral dip domain which is based on fracture angle of rocks when put under such a high horizontal stress.

Once the cross sections were completed, a minimum shortening for the mountain range up to that point in the hinterland was calculated. This was done by taking the J8 section and measuring its initial length and subtracting by the final length.

The final 3D model enables the viewer to immediately see lateral relationships in the fold and thrust belt that a traditional 2D section could not provide. The model allows for chronological modeling, seeing the order of faulting and folding.

Towards the hinterland in cross section D-D' the upper to lower Tertiary terminate at the first main thrust, suggesting a local detachment at the Tertiary/cretaceous interface (see Figure 10). Due to the first thrust fault lacking lateral continuity directly to the southeast, and far to the northeast, I do not consider this fault to be the main fault which was responsible for the most displacement. Instead, the thrust steps down to flat, and intersects the second thrust fault, the major fault in this region. It is interpreted that the major fault is a break back sequence with the more foreland fault. In sections C-C' and D-D' it is especially clear that the second thrust is cutting across sections, decapitating part of the Cretaceous seen in yellow (Figure 10 and 11). Imbricates in the hinterland were interpreted to be a break forward sequence. This is true due to the steepness of beds in the hinterland. Some beds are so steep that they are clearly refolded by the thrust fault that broke in front of it. The refolding was calculated by estimating the dip at the surface with our surface attitudes, and then extended to depth using the spectral dip domain. Each fault in the imbricate system is folded a dip order higher than the more foreland fault.

In cross section B-B' under Roca de Benet there is a well exposed J8 anticline with unconformable T23 units displaying a fanning of dip on top. This surface data leads us to believe that the geometry of the thrust sheets are being dominated by the late deep thrust sheet. It is possible that the surface J8 anticline is due to a minor fault bend fold as well. However, the first thrust sheets display very steep beds, and if, considered to be a break back sequence, must have been refolded to such an angle by a late fault. In cross section A-A' a similar J8 fold is seen at the surface, where the fault cuts across the underlying section, suggesting a break-back system with a minor fault, combined with the deep refolding, being responsible for the small anticline.

Shortening Estimates

Shortening is the amount of horizontal displacement that occurs in a mountain range after being deformed. The shortening is the difference between the initial length (l_o), and the final length (l_f). An estimated shortening for each of the four cross sections was calculated by measuring the length of the J8 bed in each thrust sheet, which is the initial length of the undeformed rocks. The final length was measured for each cross section from a given distance outboard of the frontal fold, back to the hinterland edge of the section. To calculate a shortening percent, the difference between these two lengths are divided by the initial length (l_o). From cross section A to D, the shortening in meters was 10,792m, 13,792m, 11,846m, and 11,237m respectively. From cross section A to D, the shortening percentages came out to be -57%, -65%, -61%, and -57% respectively (Table 1). Since the cross sections end about two-thirds into the hinterland, these shortening estimates would probably differ if the section were interpreted into the coastal plains. Since more deformation

occurred in the study area than further into the hinterland, the estimates will probably be slightly lower. This can be seen due to higher frequency faults in the study area and lower frequency faults further in the hinterland.

Conclusions and Future Work

The rocks in the hinterland of the cross sections have clearly not been extended all the way down to the detachment level. While constructing the sections it was clear that the rock units could not be brought down so far over such a short horizontal distance. All thrusts in a given area step up at approximately the same angle, and layer-parallel slip in a thrust sheet is limited to that caused by changes in dips of the beds (Suppe, 1985). Also, it would not make sense to bring the units down to the detachment level since deformation continues further back into the hinterland.

Though not completely balanced, the completion of four regional cross sections allows me to use an iterative approach to improve and complete the sections. By moving the sections into 3D I can view the sections stitched together as a 3D model. This allows me to see lateral variations in the thrust sheets. Any problems in the cross sections become very obvious when moved into a 3D model. This allows me to move the sections back into 2D where the problem can be fixed, and again viewed in 3D. This iterative approach would allow for the future work of finishing the sections back to the undeformed eastern edge of the Catalans. Shortening estimates could be updated, and the 3D model rebuilt. Eventually the cross sections

could be retrodeformed to the undeformed state. This would also be possible in the 3D model.

With the well constrained surface data it would be hard to suggest a better cross section interpretation that is as consistent with the regional tectonics. This comes from not only the surface constraints, but also the construction techniques that allow the section to be built as close to balanced as possible. When working in a 3D environment, after building the cross sections, it is important to remember a couple guidelines. The 3D environment is frustrating at times because it is very easy to lose a perspective. For this reason it would be discouraged to edit the sections within a 3D environment. The 3D environment provides an advantage in terms of viewing the lateral component of the region. This allowed the cross sections to provide insight on the entire region along with how the region varies laterally. In regions with such complex tectonics a single sections would not provide enough insight to the mountain belt as a whole.

REFERENCES

Burbank, Douglas, A. Meigs, N. Brozović. (1996*). Interactions of growing folds and coeval depositional systems.* Basin Research, v. 8: 199-223.

Cabrera, L., Colombo, F. & Robles, S. (1985*). Sedimentation and tectonic interrelationships in the Paleogene marginal alluvial systems of the SE Ebro Basin: transition from alluvial to shallow lacustrine environments.* In: Excursion Guide Book of the 6th European Regional IAS Meeting, Lleida (Ed. By M. Milá & S. Rosell), pp. 393-492. Institut D'Estudis, Ilerdencs, Lleida, Spain.

Calvet, F., Ramon, X. (1987*), Estratigrafia, Sedimentologia y Diagenesis Del Muschelkalk Inferior De Los Catalanides*, Depeartamento de Petrologia, Geoquimica de Geologia. Universitat de Barcelona.

Connors, Christopher D., *Undeforming a Mountain* (abstract), proceedings of XXXII International Geological Congress

Coppersmith, Ryan T., Dewhurst, Andrew D., Connors, Christopher D., (2005), *3D Structural Modeling Using Remote Sensing Data and Ground-Based LIDAR Data*. Geology Department, Washington and Lee University.

Deneba Canvas X (2005). Canvas v.10

Earth Decision Science. (2003). GOCAD. 2.0.8pl Release 2.0.8pl

Environmental Systems Research, Inc. (2003). ArcGIS 8.3

Global Mapper Software LLC, (2004-2005), Global Mapper v6.09

InnovMetric Software Inc. (2005). PolyWorks

Jones, Merren A., Paul L. Heller, Eduard Roca, Miguel Garcés, and Lluís Cabrera. (2004). *Time lag of syntectonic sedimentation across an alluvial basin*: theory and example from the Ebro Basin, Spain. Basin Research, v. 16: 467-488.

Lawton, Timothy F., E. Roca, and J. Guimerà. (1999). *Kinematic-stratigraphic evolution of a growth syncline and its implications for tectonic development of the proximal foreland basin, southeastern Ebro basin*, Catalunya, Spain. GSA Bulletin, v. 111 (3): 412-431.

López, F., A. García, A. Barnolas, A. Simó, J. González, F. Calvet, and L.Granados. (1985). Horta de San Juan: Instituto Geológico y Minero de España, Mapa Geológico de España 496, scale: 1:50000, 41 p.

Optech ILRIS 3D. (2004). Optech Incorporated. 100 Wildcat Road Toronto, Ontario Canada M3J 2Z9

Shaw, John H., C. Connors, and J. Suppe. (2004). Seismic Interpretation of Contractional Fault-Related Folds. An AAPG Seismic Atlas. Studies in Geology #53.

Suppe, John. (1983). Geometry and kinematics of fault-bend folding. American Journal of Science, v. 283: 684-721.
Journal of Science, v. 283: 684-721.

Suppe, John, Boyer E., Steven, Woodward B., Nicholas. (1985) An Outline of Balanced Cross-Sections. University of Tennessee Department of Geological Sciences Studies in Geology 11, 2nd Edition.

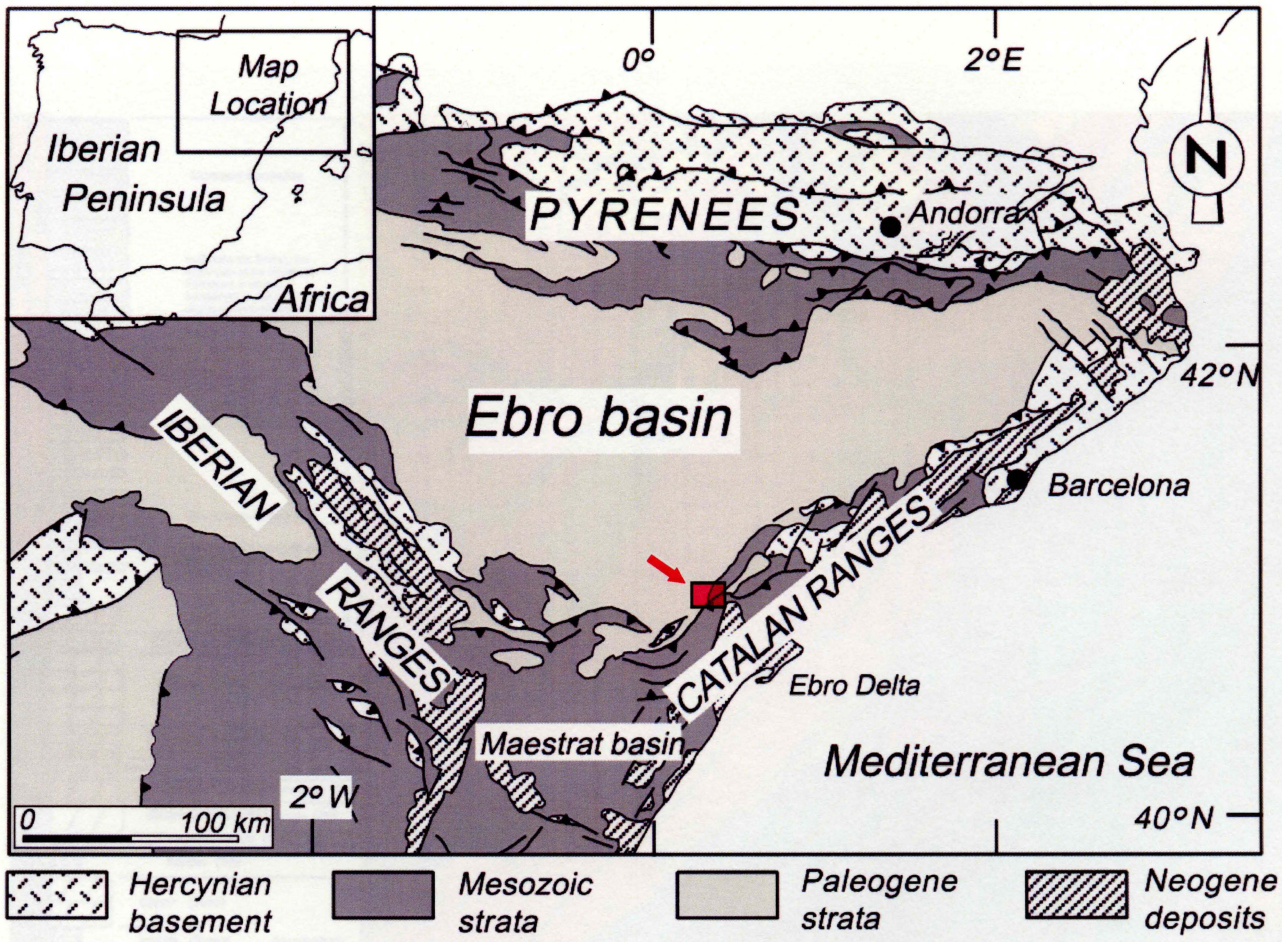

Figure 1: The three major thrust belts surrounding the Ebro Basin: the Pyrenees, the Iberian Range, and the Catalan Coastal Range. Uplift began in the early Eocene-Oligocene with the Iberian plate (peninsula) converging with the Eurasian plate. (Modified from Lawton et al., 1

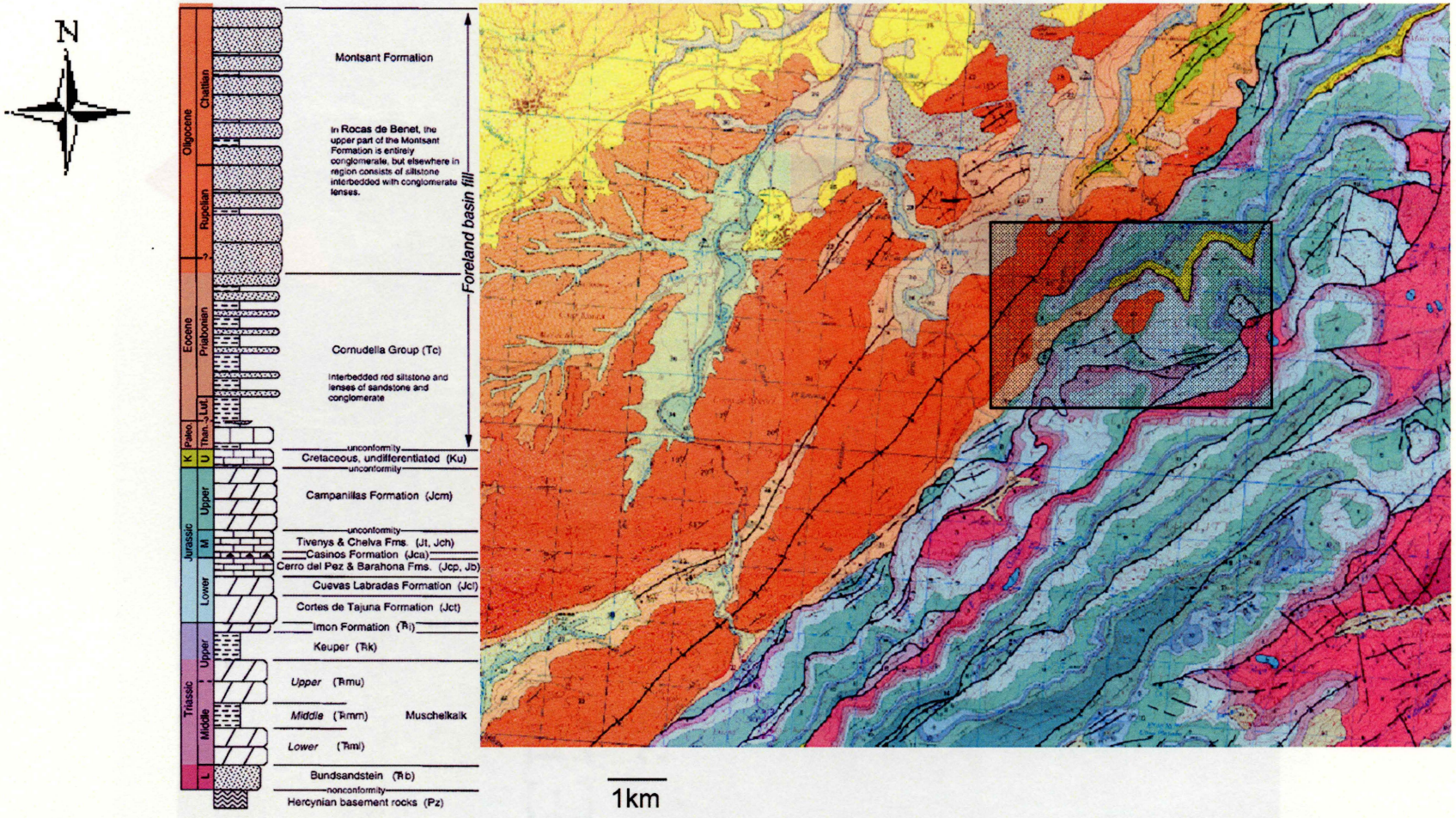

Modified from Lawton et al., 1999

Modified from Lopez et al., 1985

Figure 2: Our study area near Horta de San Joan: the margin of foreland thrusting of the Catalan Coastal Range and the basin deposits of the Ebro Basin. The oldest units exposed here are of middle Jurassic age. The orange Tertiary conglomerates represent prograding alluvial and fluvial material deposited syntectonically.

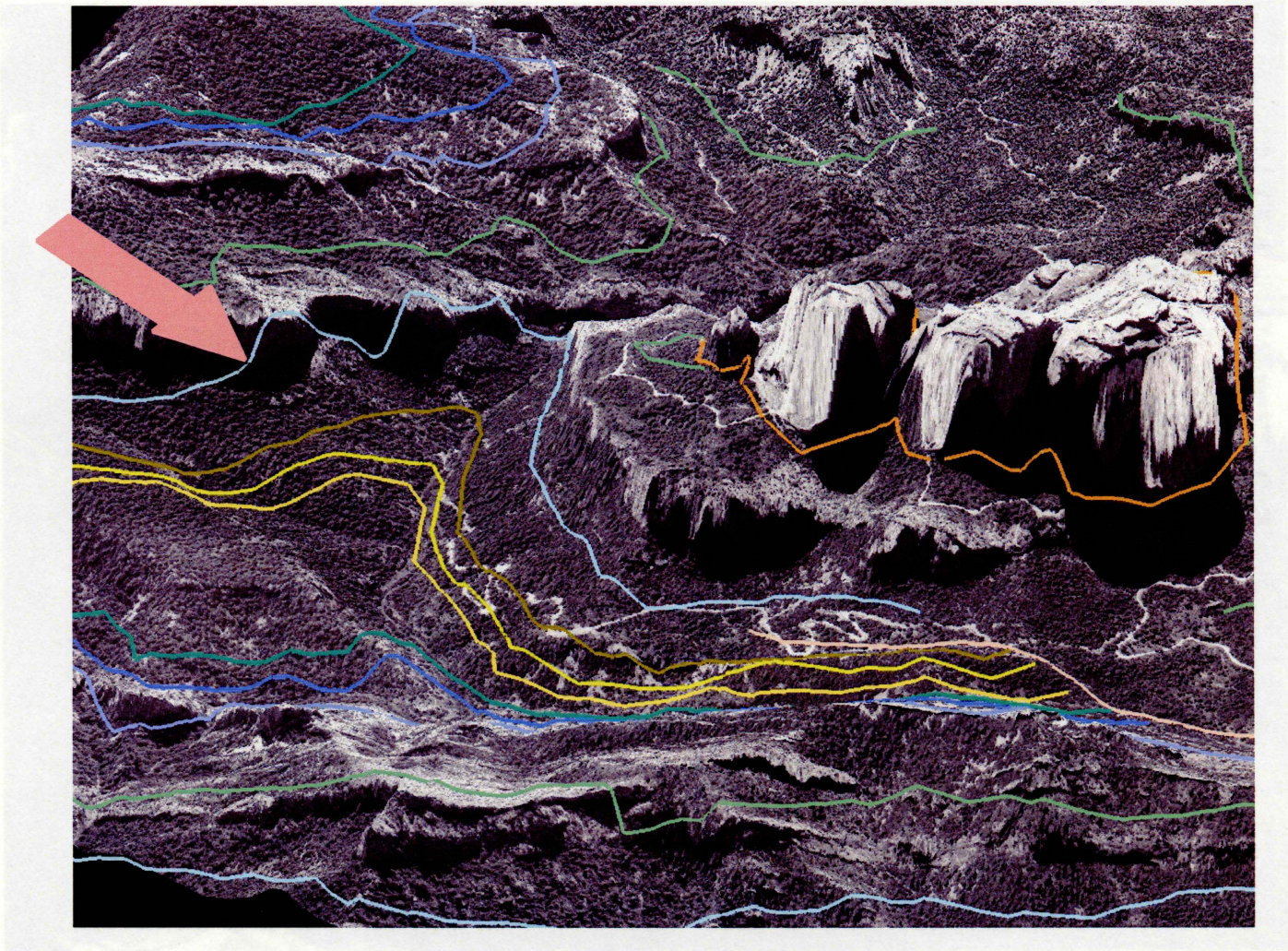

Figure 3: When the digitized geologic contacts are draped onto a 3D othophoto there are many errors. In this case the contact (see arrow) is climbing up and down a cliff face when the cliff is obviously the same geological unit.

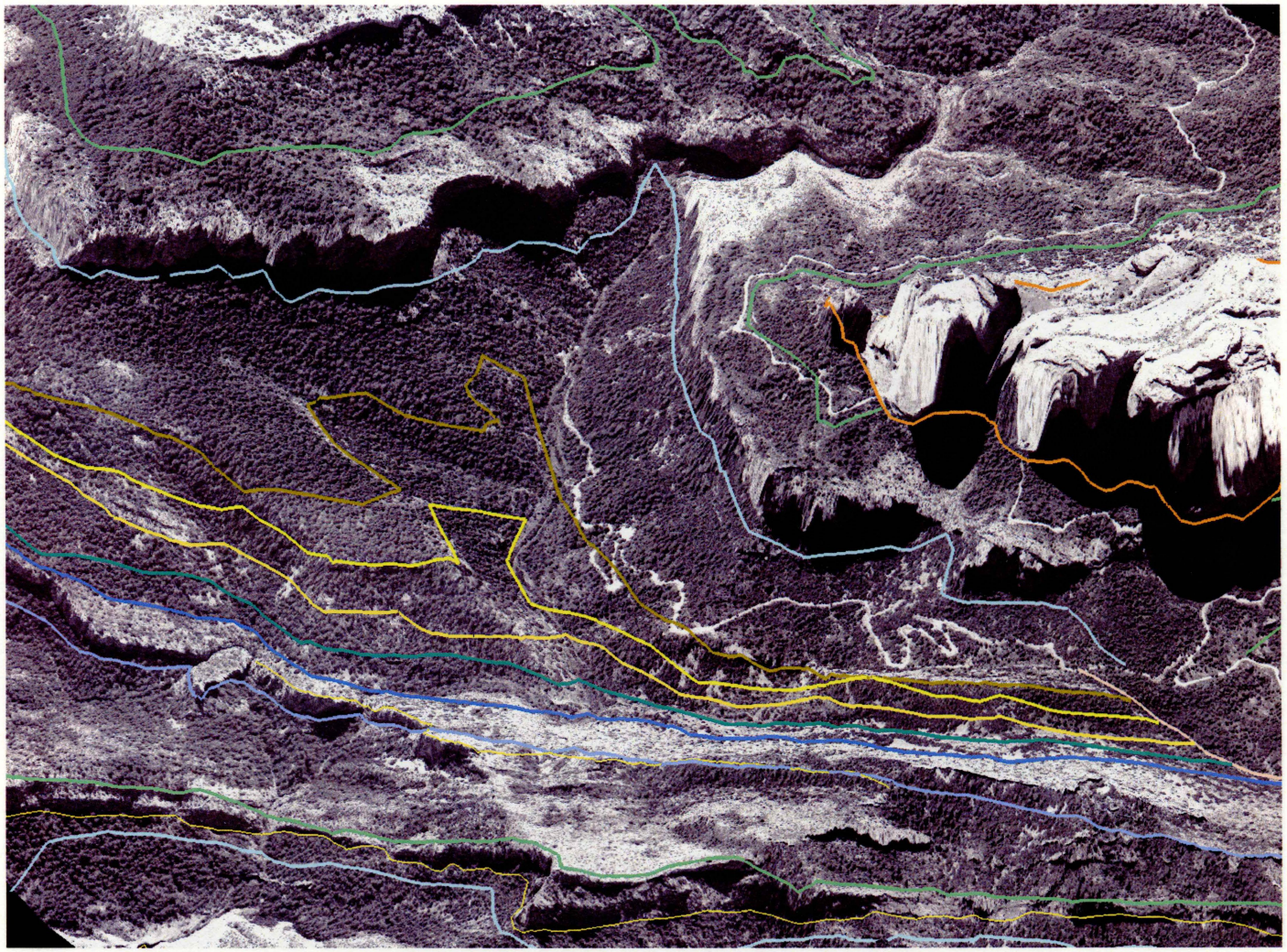

Figure 4: The contacts were corrected by mapping is ArcGIS. ArcScene is capable of viewing the data in 3D while the contacts could be edited within the 2D ArcMap.

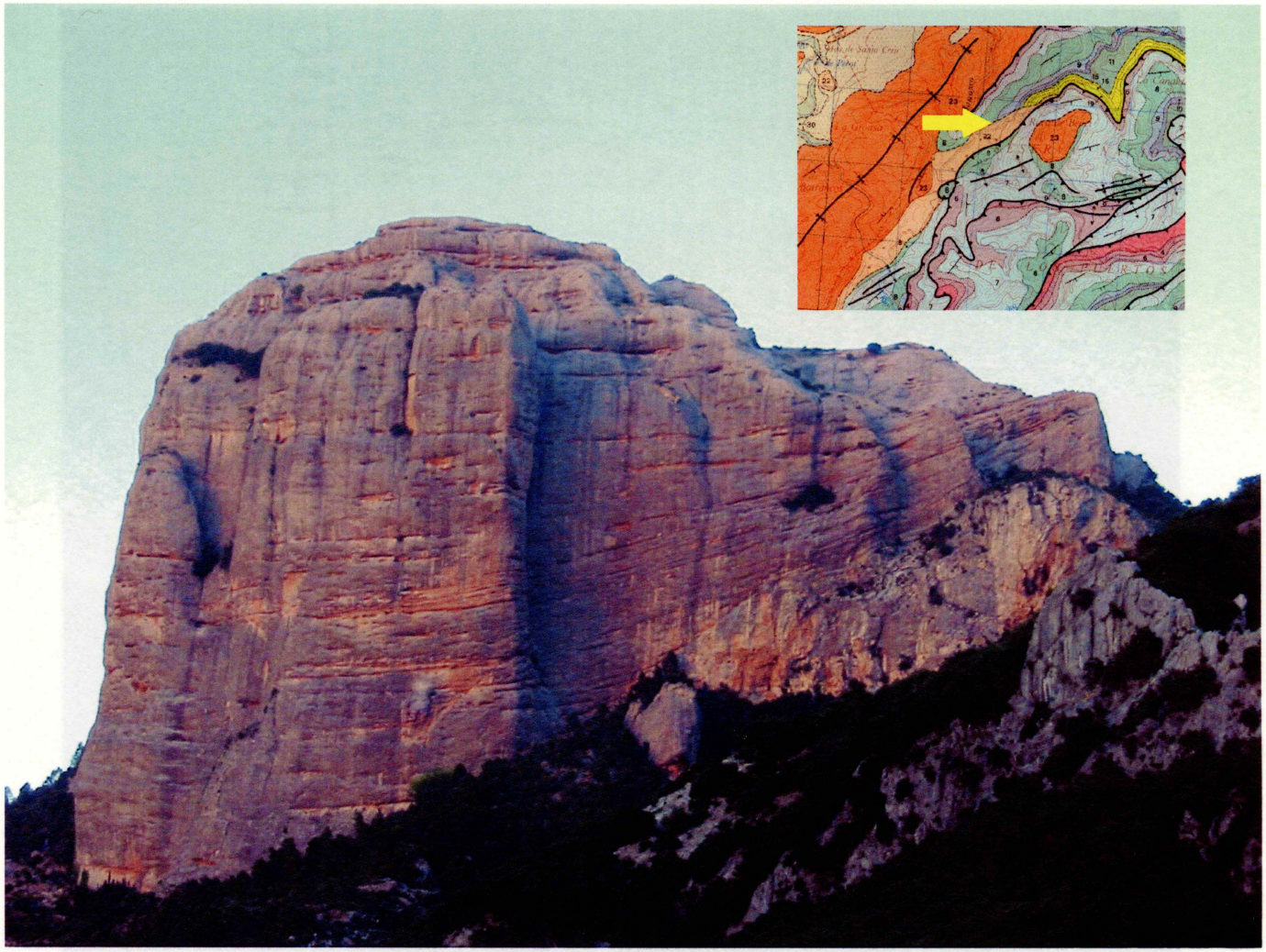

Figure 5: Roca de Benet, a prominent cliff face of growth strata sits unconformably over thrusted Jurassic pregrowth. Fanning of dip can be seen in this photo as bedding becomes steeper to the right (south).

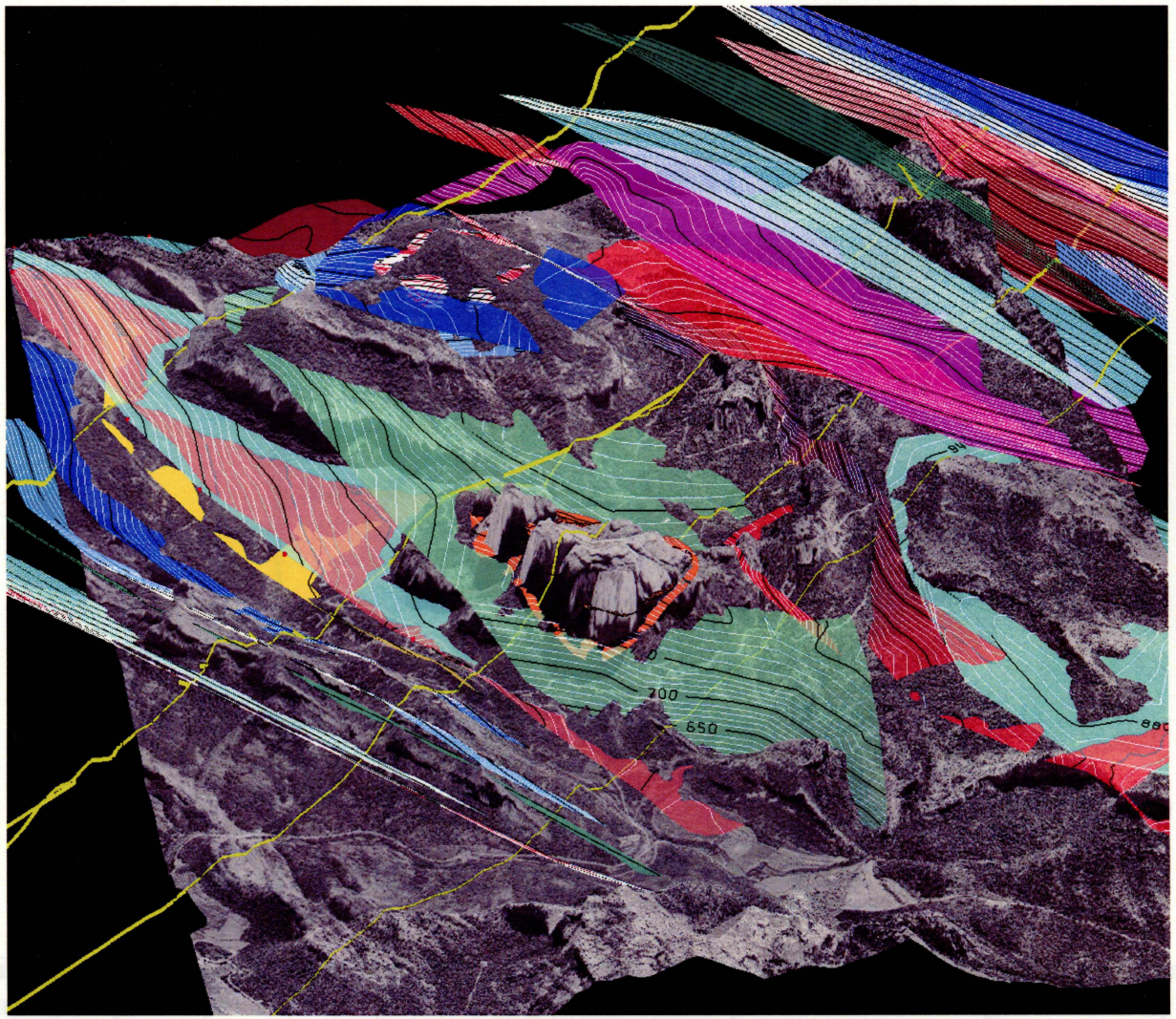

Figure 6: A surface was constructed for every contact and fault in the study area. The result is a surface attitude that extends into the air and a preliminary interpretation of the subsurface.

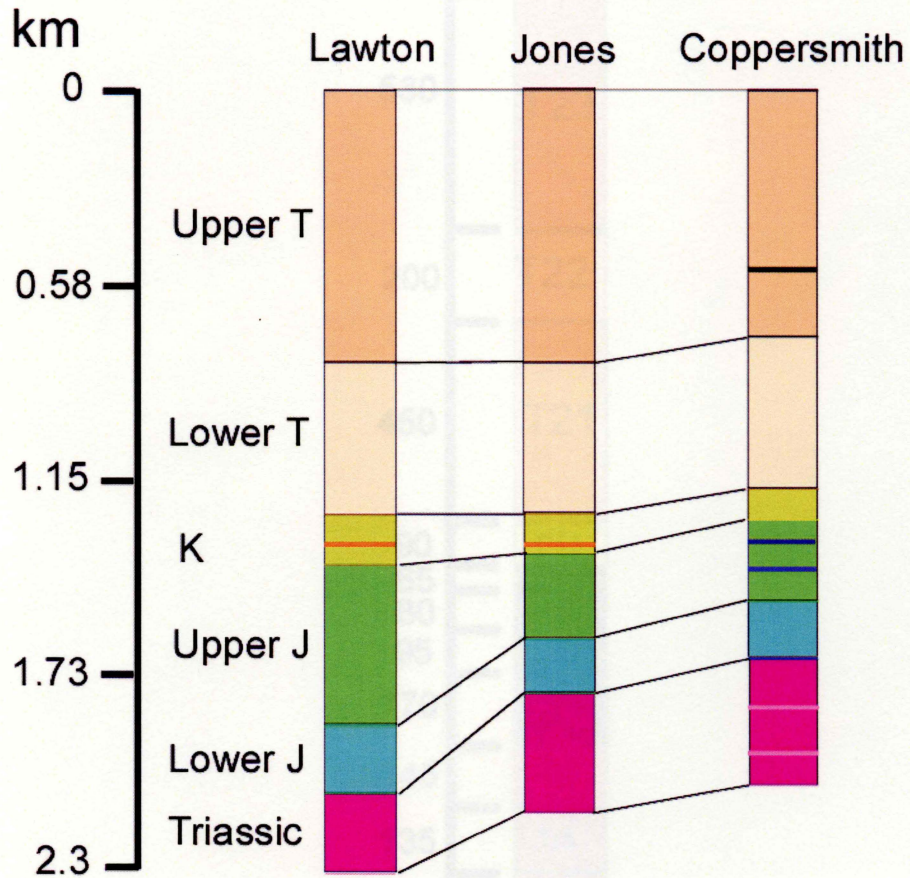

Figure 7: The stratigraphic columns of Jones et al. (2004), Lawton et al.(1999) and my own column show the differences in Jurassic and Cretaceous. The Tertiary is shown as a maximum thickness and is certainly not this thick throughout the study area. The Coppersmith column displays the more specific units within each larger unit used in this research(seen in various line colors), which Lawton and Jones only have for the Cretaceous.

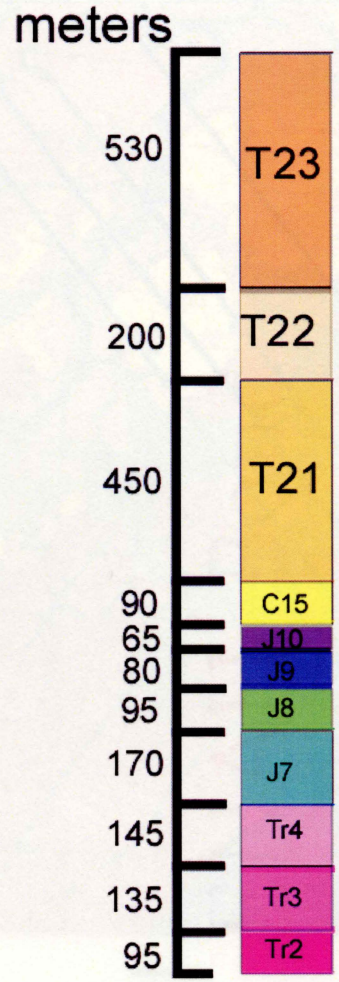

Figure 8: My stratigraphic column is categorized (consistent with Lopez et al., (1985)) from Triassic through Tertiary and labeled using the first letter of the unit followed by a number representing youngest to oldest. The numbers allow us to see the ages between units, if there is a number missing, there is an uncomformity

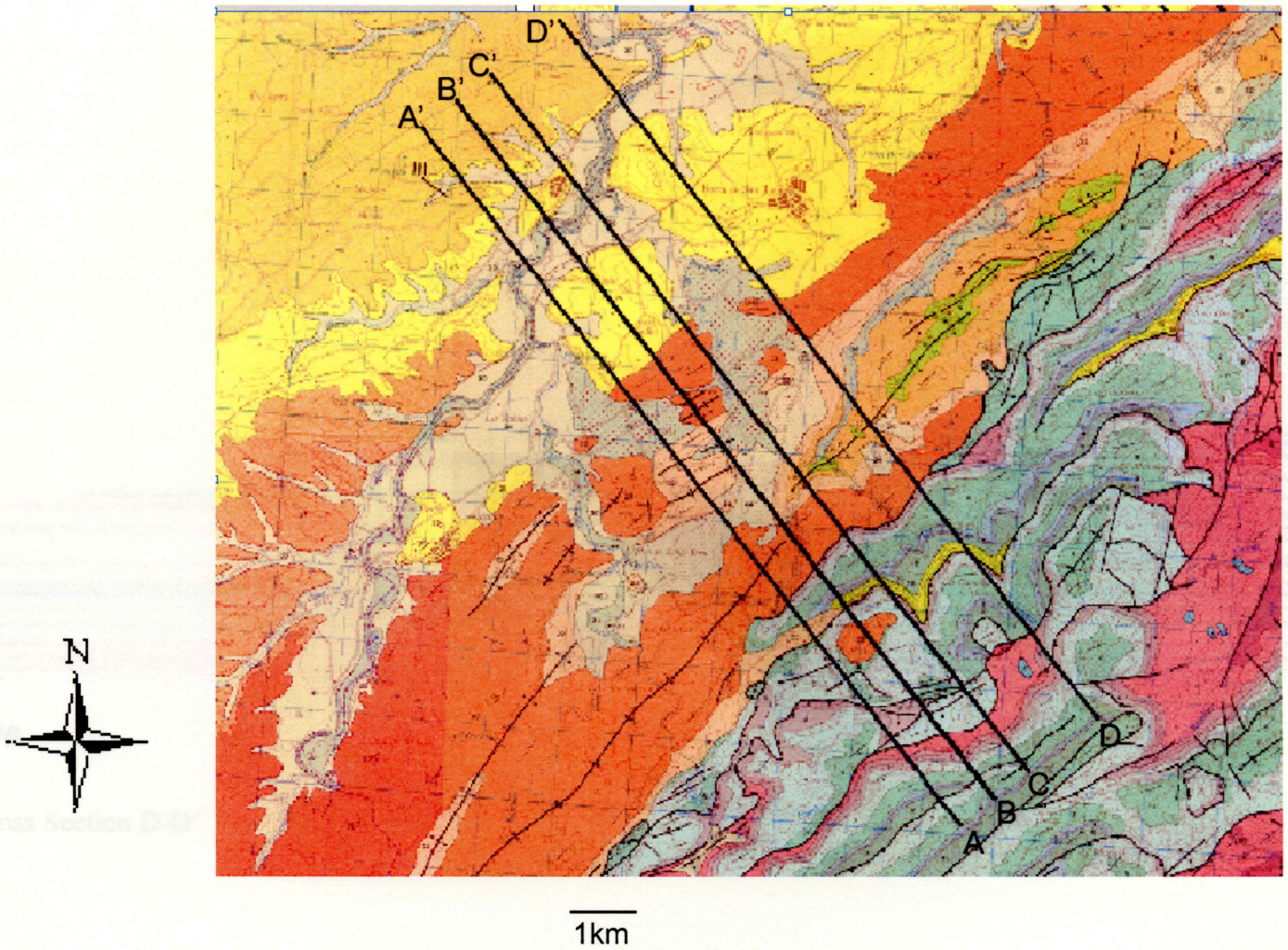

Figure 9: The four cross sections run from the southeast to the northwest. They are parallel to each other and run equal distances. Once the cross sections are constructed the close spacing will allow a 3D model to be constructed.

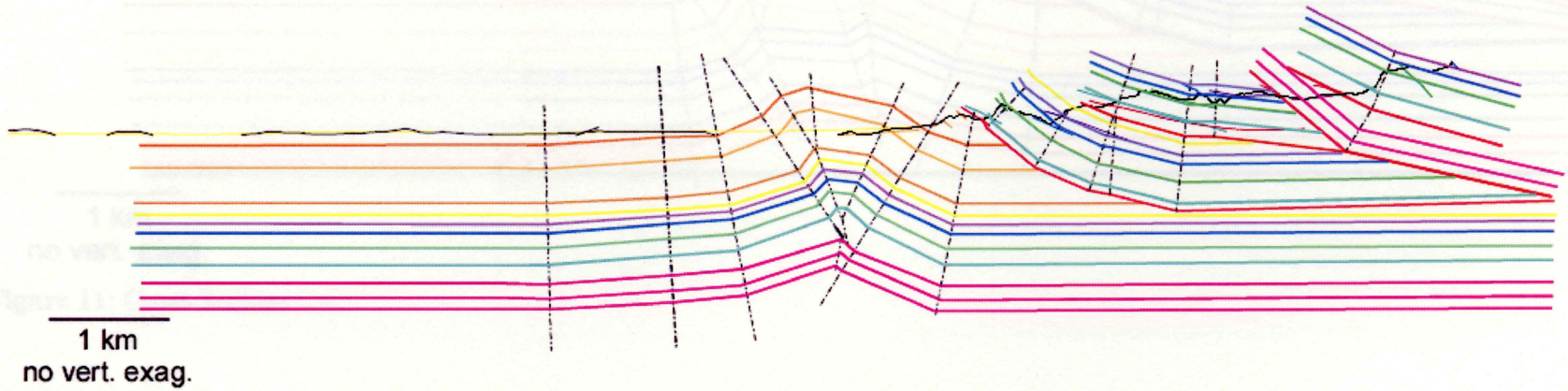

Figure 10: Cross Section D-D'

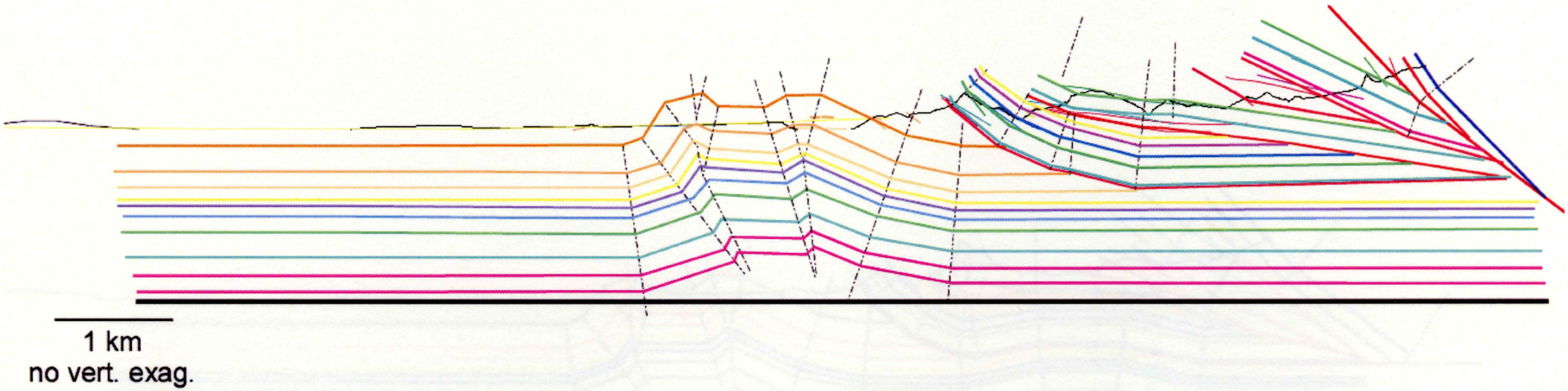

Figure 11: Cross Section C-C'

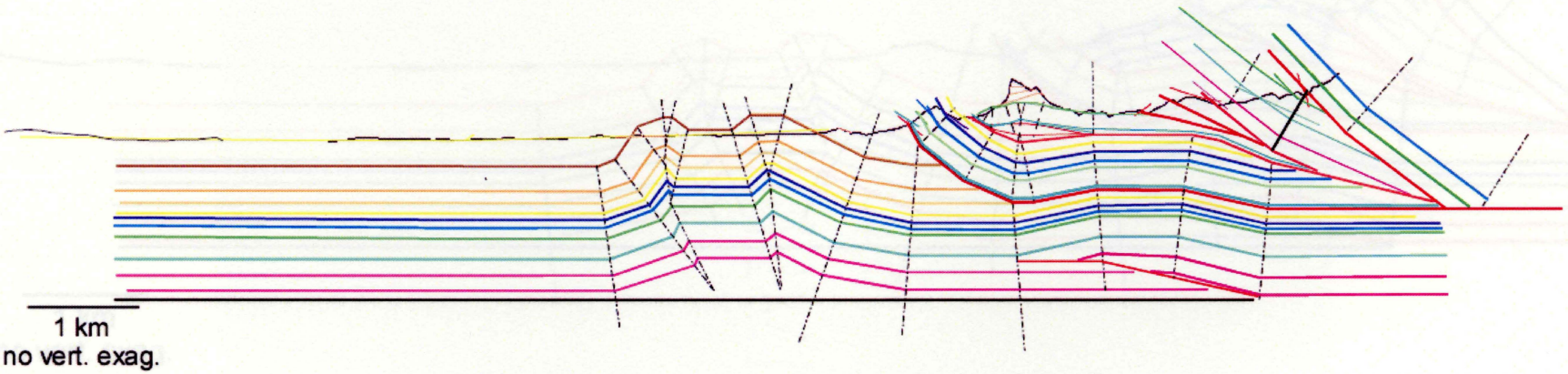

Figure 12: Cross Section B-B'

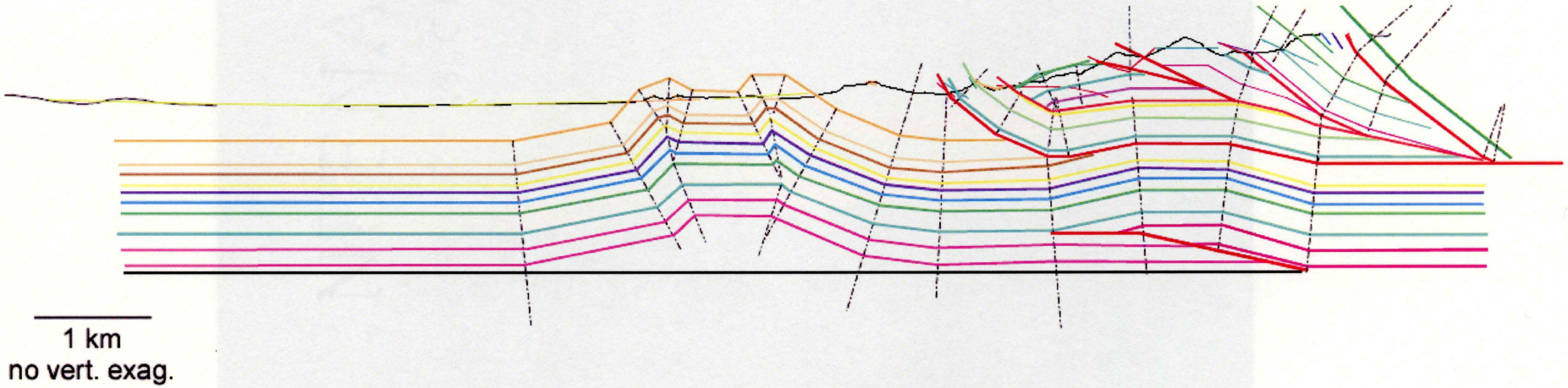

Figure 13: Cross Section A-A'

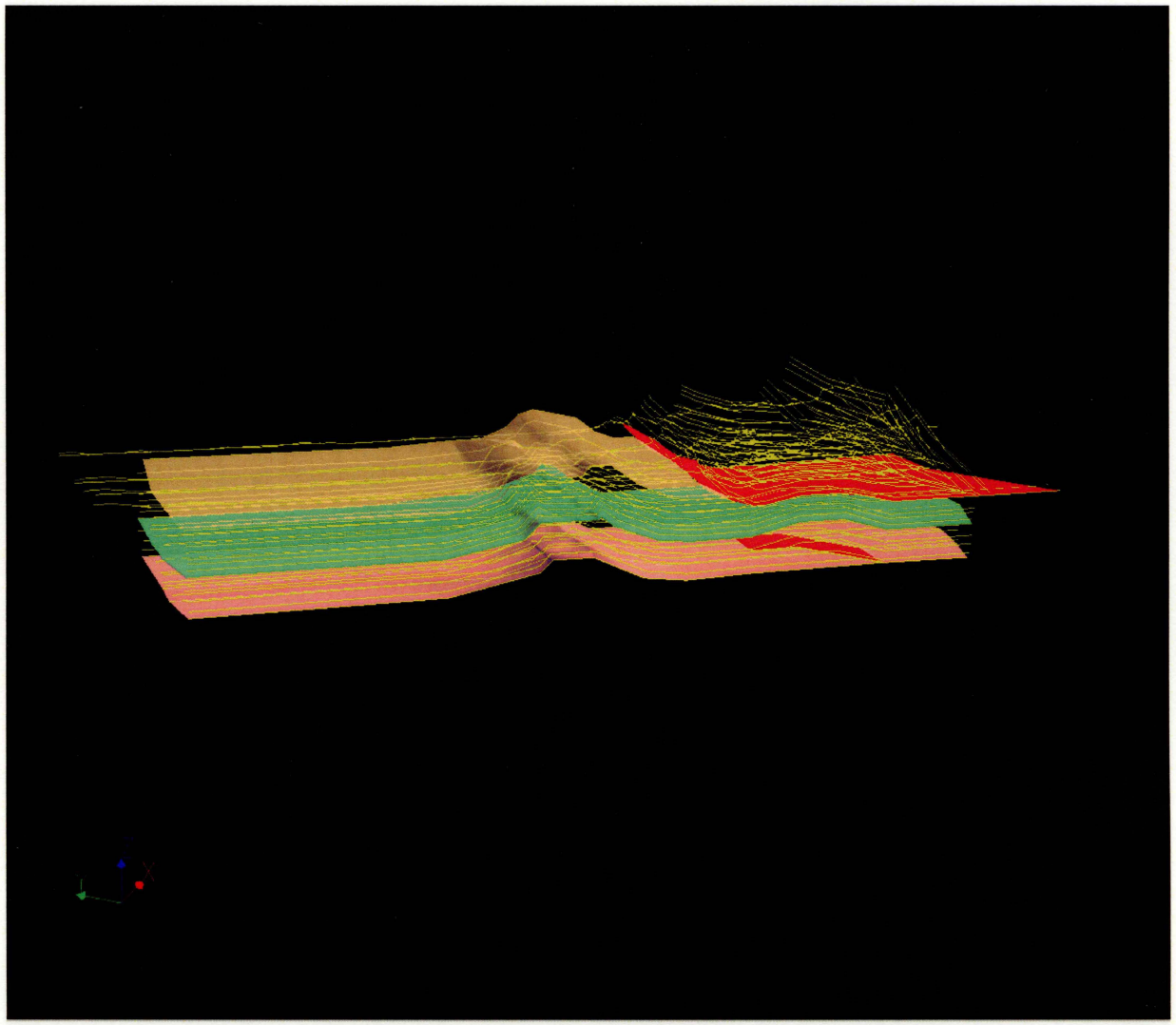

Figure 14a: 3D Model of the subsurface. All four sections are stitched together using Gocad.

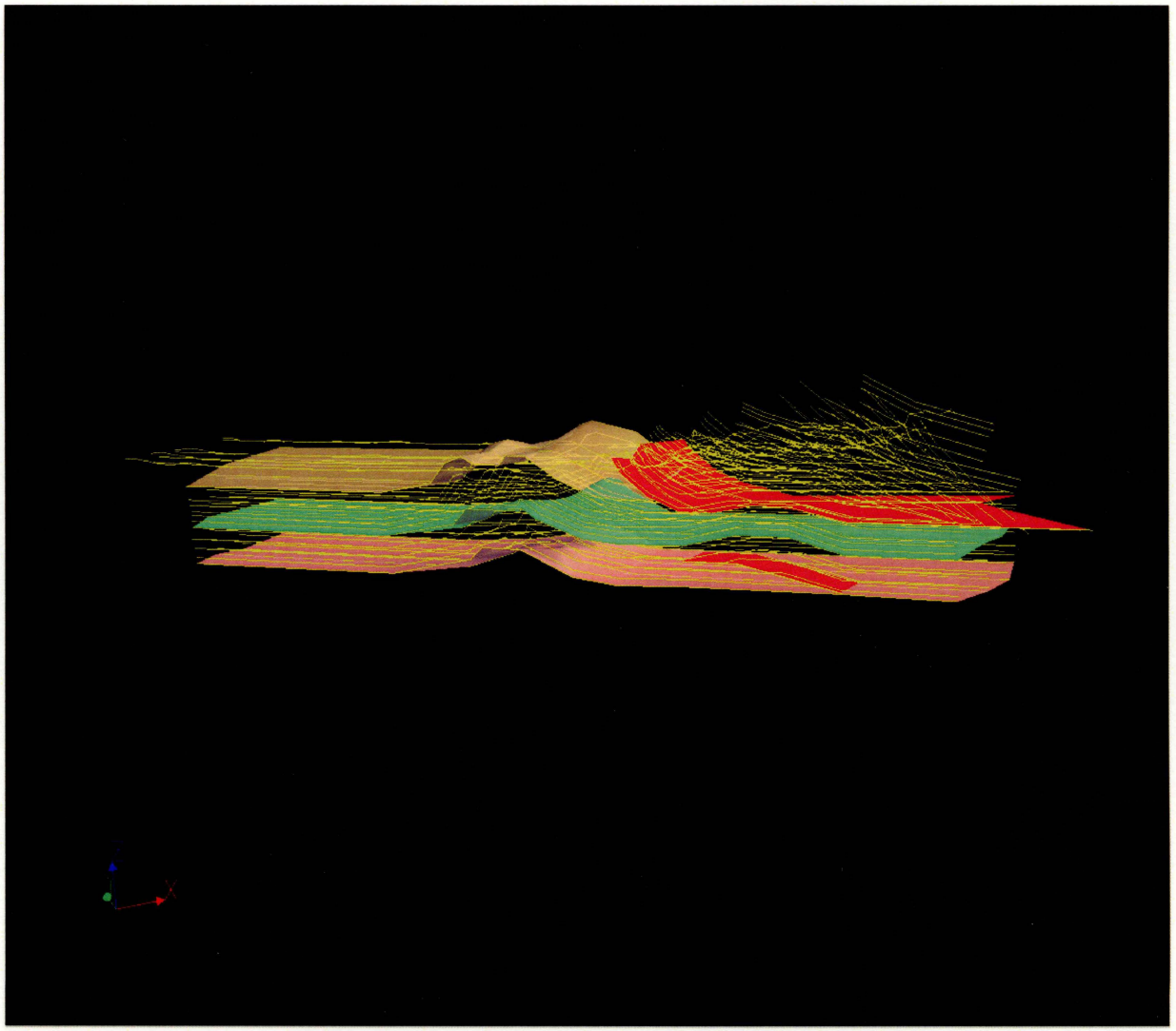

Figure 14b

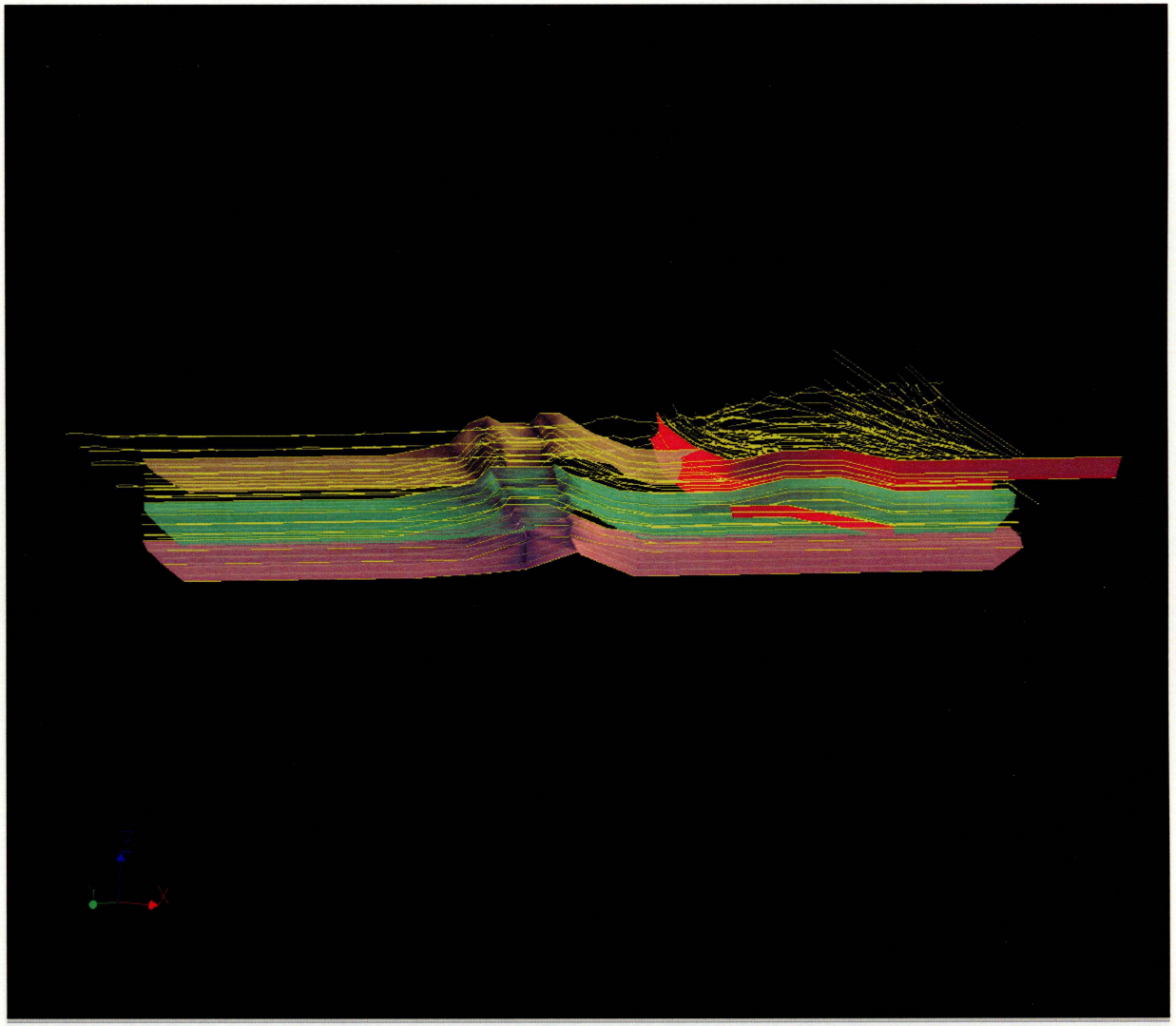

Figure 14c

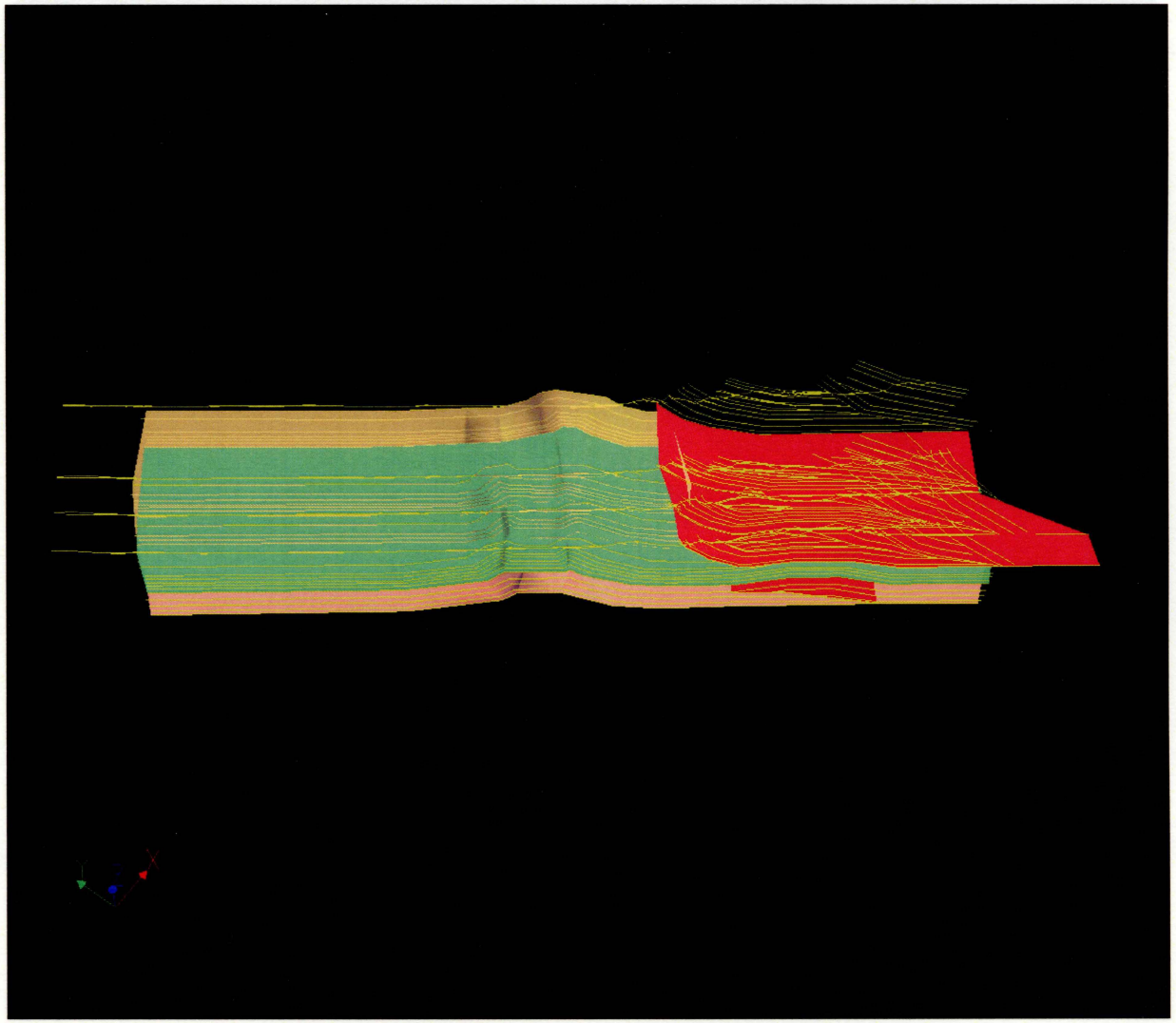

Figure 14d

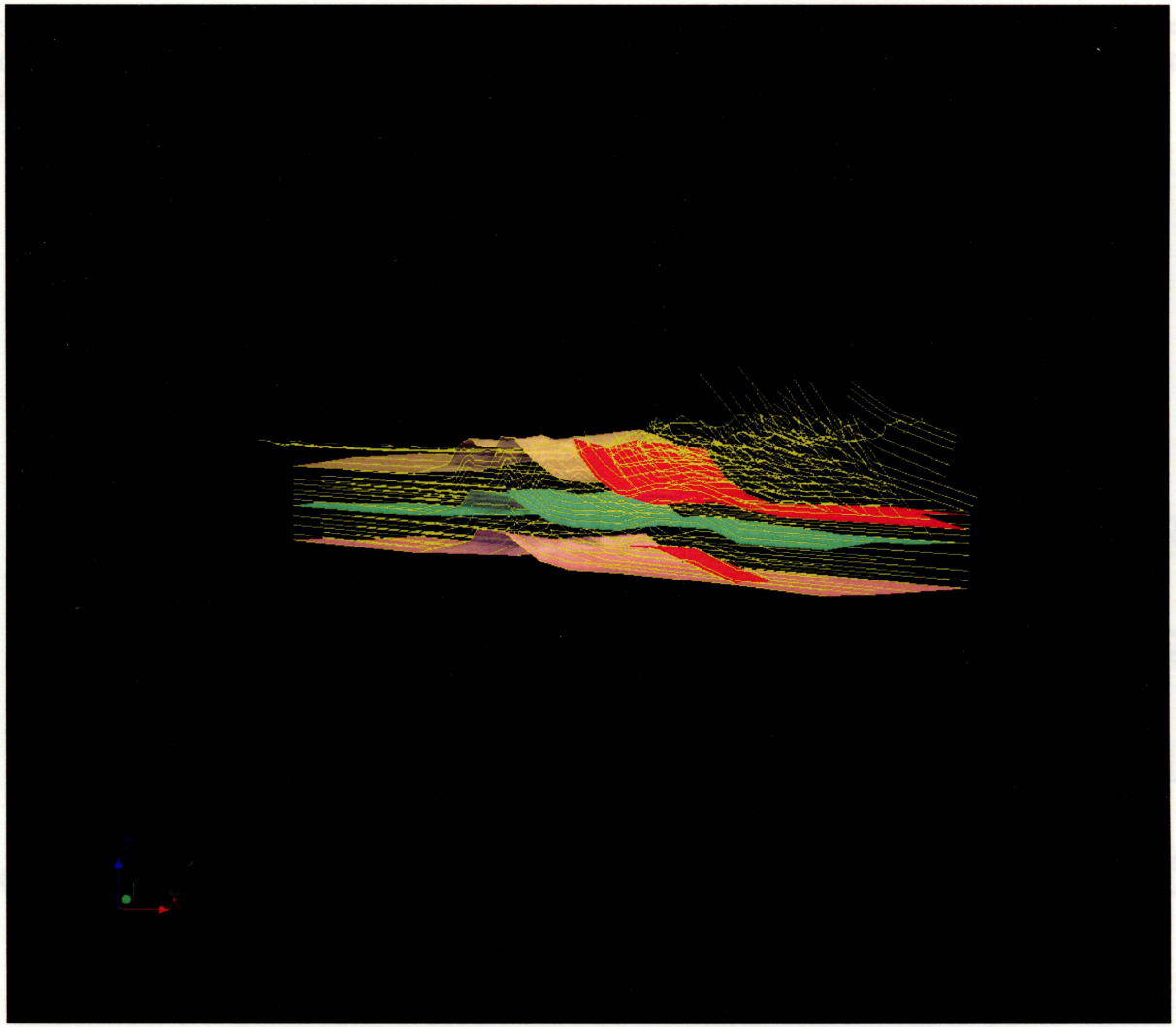

Figure 14e

Table 1: Shortening estimates taken from J08 bed. The shortening is an estimate due to the sections not being extended to the furthermost hinterland. Since the deformation further in the hinterland is relatively less than in the sections, the total shortening is most likely less than these estimates.

Shortening across central Catalan Range (m)

	A	B	C	D
lf	8195	7390	7604	8326
lo	18987	21182	19450	19563
lo-lf	-10792	-13792	-11846	-11237
(lo-lf)/lo	-57%	-65%	-61%	-57%

APPENDIX I
BUILDING GEOLOGIC CROSS-SECTIONS FROM GOCAD
MOVING PROFILES FROM GOCAD TO CANVAS

Gocad is a completely 3D environment. This workflow will demonstrate how to move between the 3D coordinate system of Gocad and the 2D system of Canvas.

Gocad works in real-world X, Y, and Z coordinates. Canvas is a 2D program that works in X-Y space. Our cross-section needed to be moved from Gocad's X-Z coordinates to Canvas's X-Y space. To do this, Chris Connors developed Matlab code to rotate and translate the lines:

To export an object that is a pline (.pl) choose File/Save Object As.

Choose the object you want to save and make sure multiple objects are not selected. Create a file name (the same name is convenient), and end the name with **(.pl).** This is important because Gocad will not recognize the object as a pline unless the file ends in (.pl). Remember to save the object to an appropriate directory. Click Save.

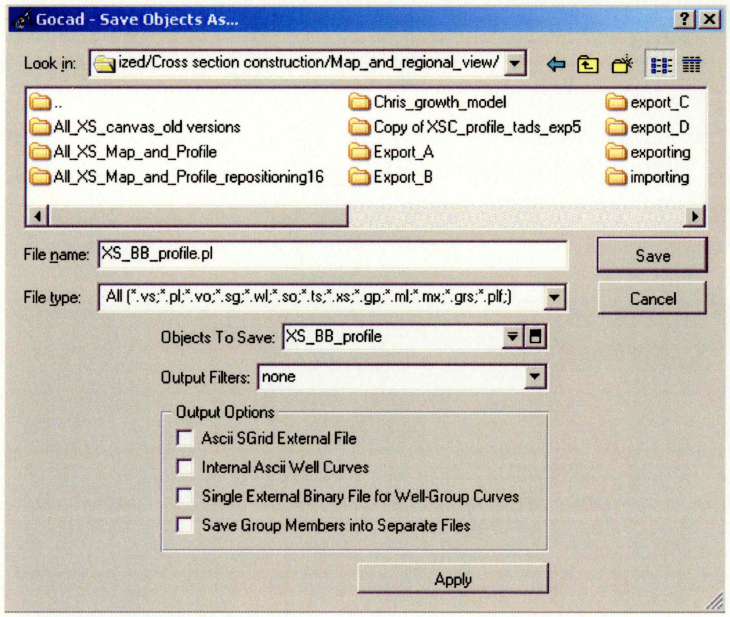

In Matlab 7.1 set the Current Directory to the folder the object was saved in. The path should already be set in this version of Matlab. If not, it should be set to: Q:\Faculty\Connors\Catalan Organized\MATLAB

Type >>ls into the command window to find the name of the pline. It is not necessary to name the shapefile with (.shp) at the end since the code automatically does this.

Use `readCatalanPlineXsecWriteShape(pline,shapefile)`

Ex)>>readCatalanPlineXsecWriteShape('XS_BB_profile.pl','XS_BB_profile.pl')

Matlab will return a unique offsetZ value for each profile. This should be recorded and must be used as an input when moving data back into Gocad. (See Appendix II for
offsetZ values).

In Canvas choose GIS/Import. Select the shapefile and click Place. The object is automatically placed in the correct coordinate system. These objects should be kept in place to allow it to be moved back to Gocad later on.

APPENDIX II
BUILDING GEOLOGIC CROSS-SECTIONS FROM CANVAS
MOVING PROFILES FROM CANVAS TO GOCAD

Profiles occasionally need to be moved from Canvas into Gocad. To move a profile from Canvas X-Y space, into GoCad X-Y-Z real world space, the presence of the Z value must be accounted for. To do this, Chris Connors has developed a matlab code that will rotate and translate the profiles into 3D space. The offsetZ value is unique to each profile and be recorded when moving from Gocad to Canvas (it will be an output in Matlab).

Many times you will not be exporting a surface profile alone. Instead, it may have multiple lines such as in a cross section. Canvas will export everything that is within the layer that is selected. To avoid confusion, use the Document Layout window (Layout/Document Layout) to deselect all other layers. The selected layer should contain objects that are to be exported, Canvas cannot export certain objects within a layer. When bringing objects into Gocad the Matlab code will rotate and translate the object from the leftmost corner of the objects in the layer. Therefore it is extremely important that the leftmost point is always the surface profile. This will allow the objects to be aligned when brought into Gocad.

To export an object from Canvas (v10), such as a full cross section to make a 3D model, choose GIS/Export. Save as type: SHP-ESRI GIS Shapefile. Be sure to save it in the appropriate directory for easy access later. Change the filename appropriately, Click Save.

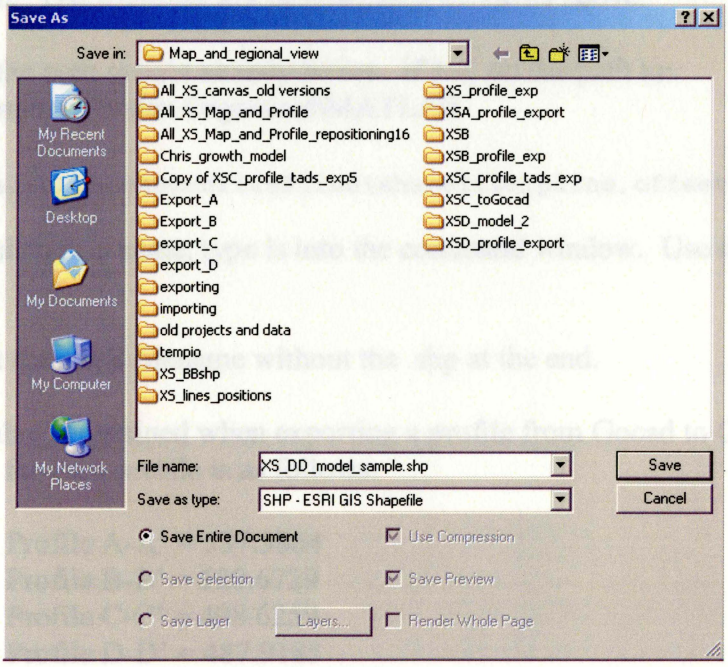

The Shapefile Export Options box will appear. Click the box in the upper left corner to select the layer you want to export. Canvas will try to export every layer within the sheet, and will export every object within the layer. The layer name was named in Canvas while the Directory name was created in the previous step. Be sure to export all objects as lines. Click OK when all options look like the box below.

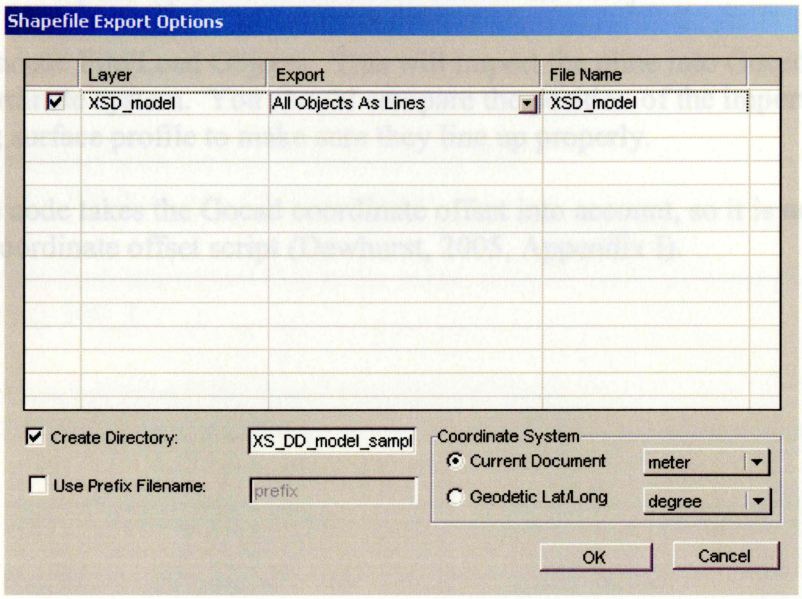

In Matlab 7.1 set the current directory to the same place you just saved the shapefile. Be sure to be within the directory that was just created, rather than the folder that the directory sits in. The file is within the directory we saved above.

In Matlab 7.1 the path should already be set. If not, set the path to:
Q:\Faculty\Connors\Catalan Organized\MATLAB

Use `readCatalanShapeXsecWritePline(shapefile,pline,offsetZ)`

To obtain the shapefile name, type ls into the command window. Use the shapefile name.

For pline input the same filename without the .shp at the end.

The offsetZ value is obtained when exporting a profile from Gocad to Canvas. The offsetZ values for each profile is as follows:

Profile A-A' = 537.5864
Profile B-B' = 528.6729
Profile C-C' = 498.6259
Profile D-D' = 487.9185

For example, I am exporting cross section D-D' (XS_DD_model_sample.shp)

>> readCatalanShapeXsecWritePline('XSD_model.shp','XSD_model',487.9185)

The file is now a pline (.pl) and saved in the current directory.

In Gocad choose File/Load Objects. This will import the pline into Gocad into the correct coordinate system. You should compare the position of the imported object to the existing surface profile to make sure they line up properly.

The Matlab code takes the Gocad coordinate offset into account, so it is not necessary to use the coordinate offset script (Dewhurst, 2005, Appendix I).

APPENDIX III
GOCAD NAMING SCHEME

A naming scheme was developed in Gocad in order to keep files organized and to avoid the build up of duplicates and old files. The naming scheme should be consistently used and, if changed, should be recorded and explained for all future users.

To name a file start with the age or name of the file.

Ex) J08 is an age, Fault is a name

If there is more than one object that is the same, number them accordingly.

Ex) J08_1

Include the name of where the object was derived from

Ex) J08_1_geomap (since it was digitized from the geologic map).

Include the type of object it is. Options include: hull, pointset (ps), pline (pl), surface (suf),

Ex) J08_1_geomap_pl or Fault_2_geomap_suf

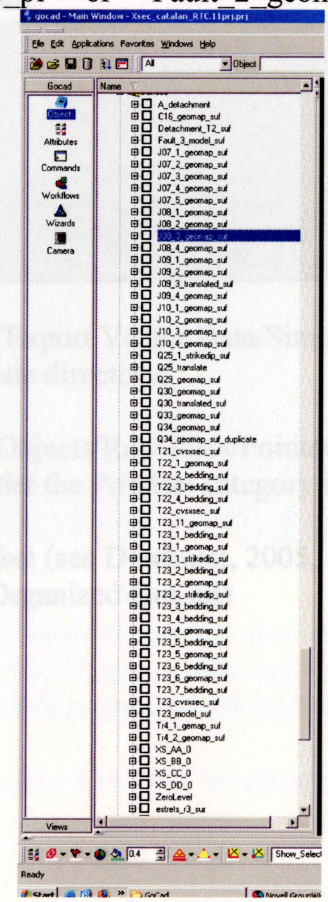

APPENDIX IV
BUILDING TIN IN GOCAD FROM GLOBAL MAPPER

Occasionally a TIN (Triangulated Integrated Network) is needed in Gocad in order to drape an existing airphoto for 3D visualization. The easiest way to do this is to build the TIN within Gocad by first exporting it from Global Mapper 6.09 (2004-05).

Load a shape file that a TIN can be built from, such as a topographic map in this directory (Q:\Faculty\Connors\Catalan Organized\Remote Sensing\Topography\5K).

Global Mapper will prompt you to choose a projection. We are working in the European Datum 1950 projection.

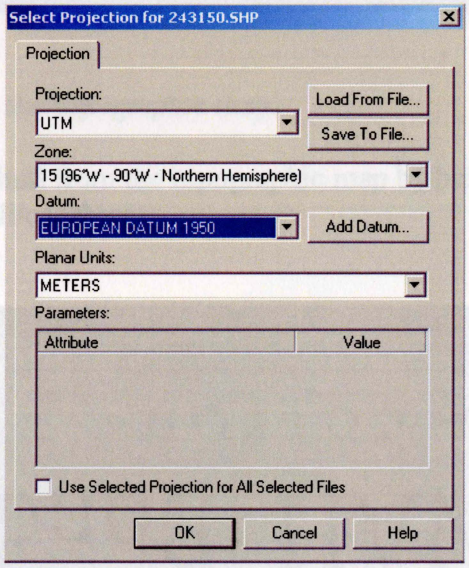

To export the file choose File/Export Vector Data/Simple ASCII Text File, click OK and Save As into the appropriate directory.

In Gocad choose File/Import Objects/Raw Files/Pointsets/XYZ ASCII File, give the file a name. It will appear under the Pointset category in the table of contents.

Set the Gocad Coordinate Offset (see Dewhurst, 2005, Appendix 1, script is saved in Q:\Faculty\Connors\Catalan Organized\GoCad)

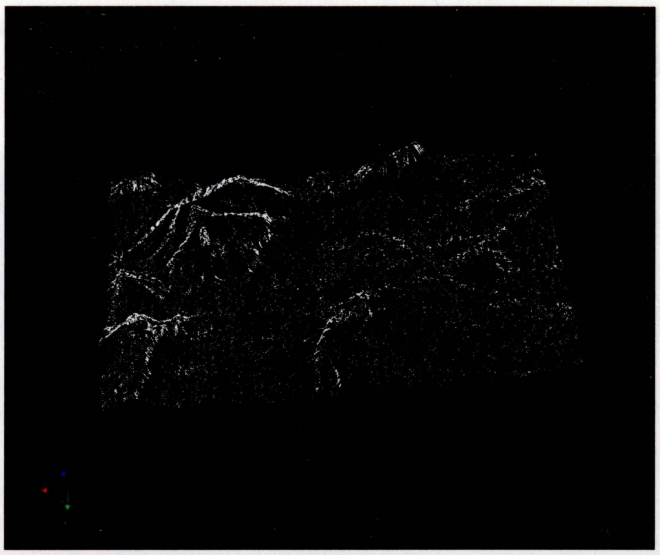

To create a surface from the topographic map:

Create a convex hull from the topographic map by being in Curve Mode, New/Convex Hull/of Object

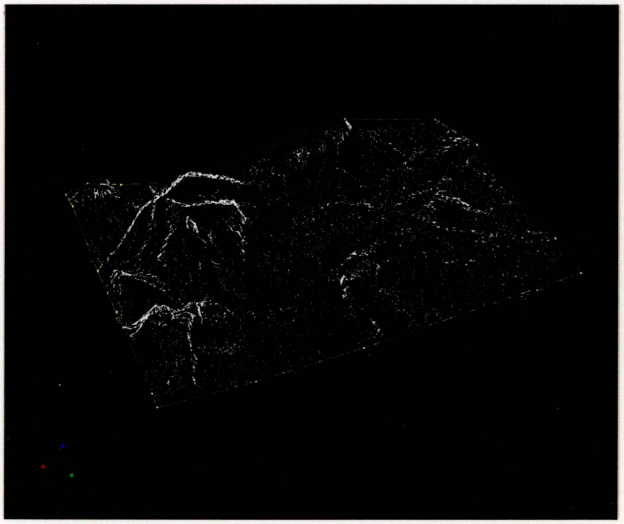

As you can see, the hull is not densified enough to cover the entire border. To fix this choose Edit/Fit to Points Globally/Apply. Click the hull with the crosshairs. Do this two or three times until the hull fits snug around the map.

Densify the Hull at approximately 50 meters by choosing Edit/Densify.

To create a surface choose Surface Mode, New/Pointset and Curve. Name the surface and click Apply, click the topo map with the cross hairs. If done correctly, the result should be a 3D surface.

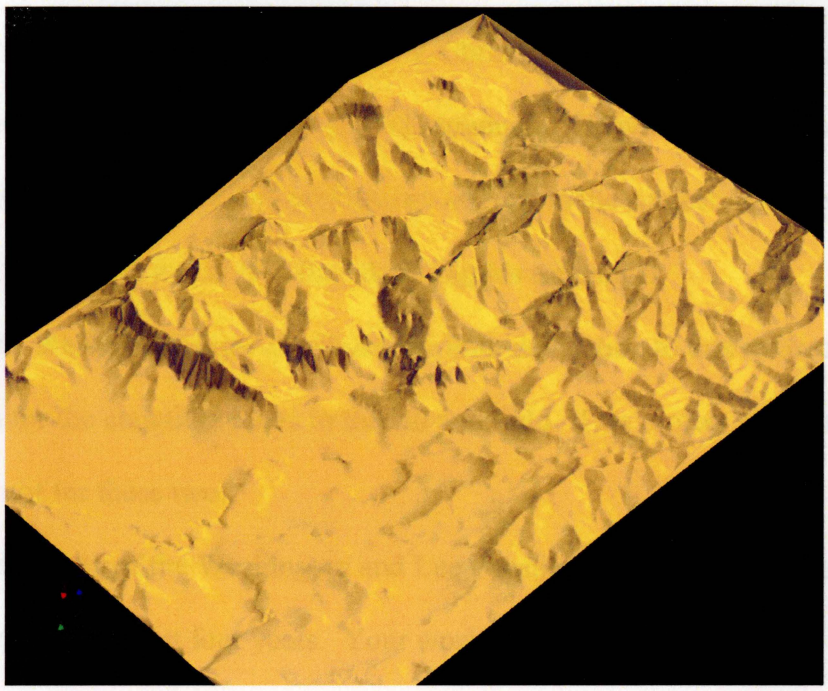

Acknowledgements

I would like to thank my advisor Dr. Chris Connors for the opportunity to work on such advanced research as an undergraduate. He was my first geology professor and is responsible for sparking my interest in the subject. He spent endless hours with me on this research in the lab during his sabbatical.

Neth Walker and Andy Dewhurst for their dedication to this research project. Thank you for the countless hours in the lab and field. This project would not be near finished if not for these two.

The faculty of the Washington and Lee Geology Department for their hard work and efforts the past four years. Your work ethic and motivation have prepared me well for my future as a geologist.